Rigid-ion potentials for SrF$_2$, CaF$_2$ and GdF$_3$

Rigid-ion potentials for SrF_2, CaF_2 and GdF_3

D Bingham†, A N Cormack‡§ and C R A Catlow‡‖

† Division of Applied Physics, CSIRO, Lindfield, Sydney 2070, Australia
‡ Department of Chemistry, University College, London, UK

Abstract. Rigid-ion potentials have been developed for CaF_2, SrF_2 and GdF_3 which predict properties that agree closely with experimental data and with the results of other polarisable ion models. The method of molecular dynamics has been used to simulate the temperature variation of ionic conductivity in SrF_2 and the results are in excellent agreement with experiment. The melting point T_m of the simulated material was 1850 ± 50 K (cf T_m (experiment) = 1723 K).

1. Introduction

As a preliminary to performing a full-scale molecular dynamic simulation of SrF_2 doped with aliovalent gadolinium, we have developed rigid–ion potentials appropriate to SrF_2, CaF_2 and GdF_3. Shell model potentials exist for both SrF_2 and CaF_2 (Catlow *et al* 1977), which predict properties such as dielectric constants and Frenkel energies that are in excellent agreement with the experimental data. However, the increased number of parameters in a shell model and the fact that all the shells have to be relaxed adiabatically at each time step result in excessive computational cost in the execution of a molecular dynamic calculation. Shell model potentials are not appropriate for this present work.

Rigid-ion potentials have been found to be satisfactory in molecular dynamic simulations provided that the static dielectric constants are correctly predicted (Dixon and Gillan 1980a). In this paper, we compare the rigid-ion potentials with experimental data and with the results of the available shell models. We also calculate the temperature-dependent ionic conductivity using a molecular dynamic simulation of 96 ions. While this is a smaller number of ions than is usually used for the prediction of thermodynamic quantities, the simulation has the advantage of being fairly quick to perform; this is important when data must be obtained at a number of different temperatures. As was shown by Gillan and Dixon (1980), a 96-ion simulation of a fluorite-structured material will reproduce the experimentally observed properties, at least in a qualitative fashion.

Catlow and Norgett (1973) reported shell model parameters for BaF_2, SrF_2 and CaF_2 which were derived from fitting to experimental data such as dielectric and elastic constants and were based on a common anion–anion interaction. These potentials enjoyed good success in correctly predicting a number of bulk properties and defect energies. There were difficulties with this potential in the treatment of the second-

§ Present address: New York State College of Ceramics, Alfred University, Alfred, NY 14862, USA.
‖ Present address: Department of Chemistry, University of Keele, Staffordshire ST5 5BG, UK.

neighbour interaction and in the magnitude of the attractive term in the short-range potential. These difficulties led Catlow *et al* (1977) to re-analyse the available data, to obtain new potentials for BaF_2, SrF_2 and CaF_2 by using a more sophisticated anion potential achieved by splining the repulsive and attractive terms. The resulting refined potentials provide excellent agreement with the experimentally obtained properties of the three materials. Dixon and Gillan (1980b) have reported the derivation of a rigid-ion potential for CaF_2. We shall compare our rigid-ion data with the results of the above models. The numerical calculations presented here were performed in 1985 during the tenure of a Commonwealth Scientific and Industrial Organisation Oversea Fellowship held by one of us (DB) and the analyses were made at a later date.

2. Potentials

2.1. CaF_2 and SrF_2

The potentials used consisted of the long-range Coulomb term, with ionic charges fixed at their nominal values, and a short-range inter-ionic contribution. This is of the form

$$V(r) = A \exp(-r/\rho) - Cr^{-6}$$

and corresponds to a Born–Mayer repulsive term and an attractive van der Waals contribution.

The potential parameters were obtained in the manner described by Catlow and Mackrodt (1982) by fitting to the experimentally observed dielectric and lattice constants which depend on the derivatives of the inter-ionic potentials with respect to the inter-ionic separation. Only the Ca^{2+}–F^- and Sr^{2+}–F^- inter-ionic potentials were refined by this procedure. The second-neighbour F^-–F^- potential was fixed at the values given by Catlow *et al* (1977). The derived potential parameters are given in table 1.

Table 1. Derived rigid-ion potentials for CaF_2, SrF_2 and GdF_3.

	A (eV)	r (Å)	C (eV Å^6)
Ca^{2+}–F^-	797.42	0.3179	0
Sr^{2+}–F^-	715.41	0.3422	0
Gd^{3+}–F^-	740.0	0.3495	0
F^-–F^-	1127.7	0.2753	15.83

2.2. Gd^{3+}–F^- interaction

Since the full-scale molecular dynamic simulation, to which this present work is preliminary, is of SrF_2 doped with gadolinium, a Gd^{3+}–F^- short-range interaction was derived from the observed properties of GdF_3, using a procedure similar to that outlined above. Parameter refinement by this method, however, did not result in an unique set of potential parameters. In order to discriminate between the range of possible potential parameters, it was necessary to use experimental data for the stability of lattice defects containing Gd^{3+} in SrF_2 and CaF_2.

The extra charge possessed by the Gd^{3+} ion, over the divalent cation for which it substitutes in the fluorite lattice, requires the presence of a charge-compensating anion in order to preserve electrical neutrality. When the compensating anion is an interstitial fluoride ion, the ion may reside in a $1|1_1$ (tetragonally symmetric) cluster with respect to the Gd^{3+} ion on a $1|1_2$ (trigonal) cluster or it may be dissociated from the Gd^{3+} ion. The notation used here is that of Corish *et al* (1982), where for $i|q_r$, i is the number of impurity ions and q is the number of interstitial ions in nearest-neighbour ($r = 1$) or next-nearest-neighbour ($r = 2$) sites relative to an impurity ion.

The rigid-ion Gd^{3+}–F^- potential was observed to be sensitively dependent on the relative stability of the $1|1_1$ and $1|1_2$ clusters in both SrF_2 and CaF_2. The difference $\Delta u(1-2)$ in the association energy $\Delta u(1)$ of the $1|1_1$ and the association energy $\Delta u(2)$ of the $1|1_2$ complexes was used to select the appropriate Gd^{3+}–F^- potential. The experimentally observed value for SrF_2 was $\Delta u(1-2) = -0.05$ eV (Matthews and Crawford 1977) and the polarisable ion simulation result for CaF_2 was $\Delta u(1-2) = -0.30$ eV (Corish *et al* 1982). The sign of $\Delta u(1-2)$ for SrF_2 was observed to change as the range of potential values was traversed, while that for CaF_2 changed only in magnitude. The potential set selected and given in table 1 predicted $\Delta u(1-2) = -0.04$ eV for SrF_2 and $\Delta u(1-2) = -0.28$ eV for CaF_2.

3. Defect energies

A number of defect energies and lattice properties was calculated for both SrF_2 and CaF_2 using the potentials described above and the results are presented in tables 2 and

Table 2. Perfect lattice properties and defect energies for SrF_2 for a lattice constant a_0 of 0.578 nm. Also included for comparison are the results of Catlow and Norgett (1973), Catlow *et al* (1977) and, where available, experimental data from Catlow and Norgett (1973) and Chadwick (1983).

	Experimental value	Rigid-ion value	Value from Catlow *et al* (1977)	Value from Catlow and Norgett (1973)
a_0	0.578	0.578	0.578	0.578
ε_0	6.15	6.12		6.10
C_{11}	12.88	12.17		13.0
C_{12}	4.748	2.83		4.75
C_{44}	3.308	2.83		2.73
H_L	−25.33	−25.18		−26.37
Anion vacancy		4.11	4.80	5.57
Cation vacancy		21.57	22.09	22.13
Anion Frenkel defect	2.38–2.39	2.40	2.38	2.39
Schottky defect		4.61	5.92	6.90
Anion activation	0.52–0.58	0.15	0.43	0.30
Anion interstitialcy	0.75	0.54	0.80	0.69
Anion interstitial		−1.71	−2.42	−3.18
Gd^{3+} substitution		−21.73		−21.65
Gd^{3+}–F^- $1|1_1$		−23.98	(-0.53)[a]	
Gd^{3+}–F^- $1|1_2$		−23.94	(-0.54)[a]	

[a] Energy difference.

Table 3. Defect energies for a lattice constant a_0 of 0.6095 nm, corresponding to a temperature of $T = 0.92T_m$.

	Rigid-ion value
a_0	0.6095
ε_0	12.12
C_{11}	8.40
C_{12}	0.76
C_{44}	0.68
H_L	-24.97
Anion vacancy	4.00
Cation vacancy	19.70
Anion Frenkel defect	1.62
Schottky defect	2.73
Anion activation	≈ 0
Anion interstitial	-2.38
Gd^{3+} substitution	-21.37
Gd^{3+}–F^- $1|1_1$	-23.81
Gd^{3+}–F^- $1|1_2$	-24.14

3 for SrF_2 and in table 4 for CaF_2. In general, the agreement between the results of the rigid-ion model and those of the polarisable ion models and, where available, the experimental data were as good as may be expected. The lattice and dielectric constants are accurate, as might be expected since it was to these quantities that the potentials were fitted. The residual bulk strain, which is an indication of the stability of the lattice, was very small in both SrF_2 and CaF_2 while the lattice energies agree well with experiment. The underestimation of the anion activation energy and the elastic constants is attributable to a softening of the short-range repulsive interaction from that observed

Table 4. As for table 2 but for CaF_2, and $a_0 = 0.544$ nm. Also included for comparison are the results of Dixon and Gillan (1980b) for a rigid-ion potential.

	Experimental value	Rigid-ion value	Value from Catlow et al (1977)	Value from Catlow and Norgett (1975)	Value from Dixon and Gillan (1980b)
a_0	0.544	0.544	0.544	0.544	0.544
ε_0	6.47	6.42		6.42	5.20
C_{11}	17.124	16.55		16.9	15.8
C_{12}	4.675	3.31		4.80	4.15
C_{44}	3.624	3.33		3.23	3.96
Bulk strain		0.19%			
H_L	-26.76	-26.87		-28.06	-27.10
Anion vacancy		4.23	4.85	5.88	
Cation vacancy		23.08	23.17	23.30	
Anion Frenkel defect	2.71–2.71	2.58	2.75	2.63	2.71
Schottky defect		4.67	5.75	7.00	
Anion activation	0.38–6.47		0.35	0.20	0.19
Anion interstitial		-1.65	-2.10	-3.25	
Gd^{3+} substitution		-19.40			
Gd^{3+}–F^- $1|1_1$		-22.05			
Gd^{3+}–F^- $1|1_2$		-21.77			

in the shell models, although the relative difference between anion vacancy and anion interstitial energies is maintained. This resulted from an attempt to compensate partially for the lack of electronic polarisation. Good agreement is obtained for the anion Frenkel energies in both SrF_2 and CaF_2. The overestimation of the Schottky energy for CaF_2 is attributable to an overestimation of the anion vacancy energy in this material. The rigid-ion potential derived for CaF_2 shows closer agreement with the experimental data than does the potential reported by Dixon and Gillan (1980b); this reflects the decision to fit a larger range of lattice properties than just the lattice constant and the anion Frenkel energy.

4. Molecular dynamic simulation

The temperature variation of the diffusion coefficient was followed by the use of simulations with a system of 96 ions (64 anions and 32 cations). This corresponds to a primary box of side length two lattice constants. The small size enables a number of runs at different temperatures to be performed economically.

The method of molecular dynamics applied to ionic materials is well documented (see, e.g., Catlow and Mackrodt 1982, Sangster and Dixon 1976) and we make no attempt to present the details of the calculation here. The computer code, FUNGUS, which we used, has been described by Walker (1982) and uses the algorithm of Beeman (1976) to update the particle trajectories, i.e.

$$r(t + \delta t) = r(t) + v(t)\,\delta t + \tfrac{1}{6}[4a(t) - a(t - \delta t)](\delta t)^2$$

$$v(t + \delta t) = v(t) + \tfrac{1}{6}[5a(t) + 2a(t + \delta t) - a(t - \delta t)]\,\delta t$$

where r, v and a refer to the particle position, velocity and acceleration, respectively. The time increment δt used was 10^{-14} s, an order of magnitude smaller than the minimum vibrational period (Gillan and Dixon 1980). The long-range Coulomb sums were performed using an Ewald summation.

5. Lattice expansion

The temperature variation of the lattice constant for isostructural PbF_2 and $SrCl_2$ have been measured by Dickens *et al* (1976). From these data, we estimate a linear thermal expansion coefficient α for SrF_2 of 3.9×10^{-5} K^{-1}. We prefer this estimate to an extrapolation of the data for SrF_2 measured by Sirdeshmukh and Deshpande (1964) since it was acquired over a limited temperature region below 280 °C. Moreover the curvature of the data leads to an extrapolation of $\alpha \simeq 2 \times 10^{-4}$ K^{-1} in the temperature region of interest, $T > 1400$ °C; this extrapolation is unrealistically high.

6. Defect energies at $T = 1700$ K

The static lattice calculations used here do not include thermal vibrations. The complete effect on the defect calculations of raising the temperature can only be examined by their explicit inclusion.

We have performed some defect energy calculations for SrF_2 using a lattice constant a_0 of 0.6095 nm; this corresponds to a temperature T of $0.92T_m$ for the simulation, or a

nominal temperature T of 1700 K. These calculations are shown in table 3. The magnitude of the dielectric constant at this temperature is consistent with that reported by Rao and Smakula (1966) for CaF_2. There is a change ΔC_{11} in C_{11} between 0 and 1600 K of about 30% (Catlow *et al* 1978) which is also accurately represented, although a much larger decrease in C_{12} is observed.

A significant decrease in the binding energy of the $1|1_1$ cluster is predicted, while the energy of the $1|1_2$ cluster remains comparatively unchanged. The change in the relative stability of the clusters will be discussed in the context of the full-scale simulation in the accompanying paper (Bingham *et al* 1989).
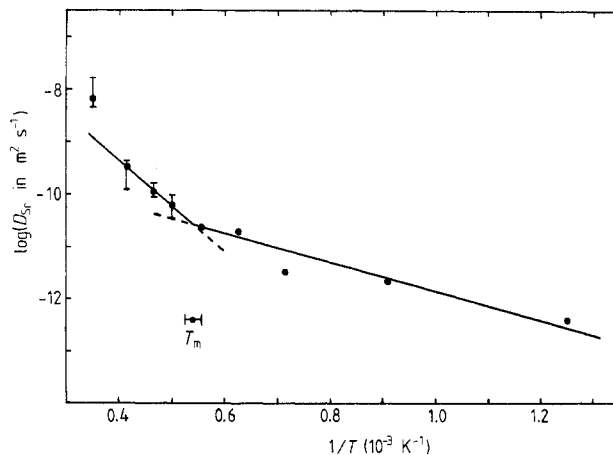
7. Diffusion coefficients

The diffusion coefficient D_α of ion species α was calculated from the time variation of the mean-square ionic displacements (Einstein 1905)

$$\langle r_\alpha(t)^2 \rangle = 6D_\alpha|t| + B$$

from which the conductivity σ at temperature T can be derived using the Nernst–Einstein relation, taking account of the ionic self-correlation effects as given by the Haven ration H_R. The Haven ratio is the ratio of the directly measured diffusion coefficient (from tracer-type experiments) to that calculated from the bulk conductivity. For the fluorite lattice, Chadwick (1983) gives $H_R \simeq 0.65$. This ratio has been uniformly applied to the data for consistency, although a different ratio probably applies above the melting point.

8. Melting temperature

The melting point T_m of the simulated material can be found from the abrupt change in the cation diffusion coefficient D_{Sr} which occurs on melting. The temperature variation of D_{Sr} is shown in figure 1. As may be seen, the small magnitude of the diffusion
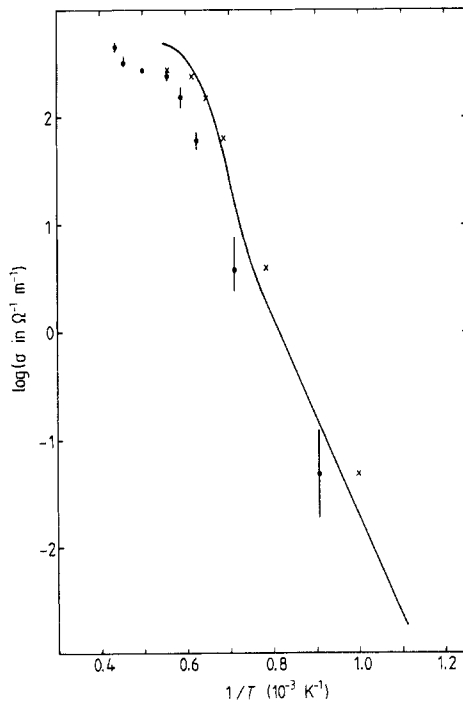

Figure 1. Temperature variation of the cation diffusion coefficient D_{Sr} for SrF_2 with inverse temperature. Error bars were calculated as shown.

coefficient below T_m allows a range of possible curves to be drawn through the data. This range, however, does not significantly affect the derived melting point T_m of 1850 ± 50 K. This is some 7% higher than the experimentally observed melting temperature (Chadwick 1983). Some elevation of T_m can be expected owing to the lack of nucleation sites within the model. Gillan and Dixon (1980) and Dixon and Gillan (1980a) have performed a simulation on isostructural $SrCl_2$ and observe transition temperatures which are too high. They attribute this effect to an overestimation by about 20% of the anion Frenkel energy. Since this defect energy is correctly predicted by our model, we do not attribute the relatively small elevation of T_m directly to this effect, although we note that the temperature variation of the entropy contribution to this quantity is not known.

9. Anion conductivity

In figure 2, we show the temperature variation of the simulated anion conductivity, corrected for self-correlation effects, together with the experimental data of Derrington *et al* (1975) (full curve). The simulated conductivity is seen to be displaced along the temperature axis from the experimental observations, which we attribute to the elevated melting point of the material. When the temperature scale of the simulated data is rescaled by the ratio T_m (experiment)/T_m (simulation), this offset is removed and excellent agreement with the experiment is obtained over four decades of conductivity

Figure 2. Simulated temperature variation of the anion conductivity for SrF_2 (●) corrected for anion self-correlation effects. Also shown for comparison are the experimental data of Derrington *et al* (1975) (———). The anion conductivity rescaled by the ratio T_m (experiment)/T_m (simulation) (×) is also given.

(see figure 2). There is a considerable margin for error, however, in the simulation results at lower temperature owing to the relatively small magnitude of the derived diffusion coefficient.

10. Summary

We have developed rigid-ion potentials for CaF_2, SrF_2 and GdF_3 which predict defect energies and lattice properties that agree well with the experimental data. Defect calculations that were performed using an expanded lattice to reflect an elevated temperature predict a significant change in the relative stability of simple Gd^{3+}–F^- clusters while predicting sensible changes in the other lattice properties. The derived temperature variation of the ionic conductivity is in excellent agreement with experimental observations, giving some assurance that the simulation results accurately reflect reality.

Acknowledgments

References

Beeman D 1976 *J. Comput. Phys.* **20** 130
Bingham D, Cormack A N and Catlow C R A 1989 *J. Phys.: Condens. Matter* **1** 1213
Catlow C R A, Comins J D, Germano F A, Harley R T and Hayes W 1978 *J. Phys. C: Solid State Phys.* **11** 3197
Catlow C R A and Mackrodt W C (ed.) 1982 *Springer Lecture Notes in Physics* vol 166 (Berlin: Springer)
Catlow C R A and Norgett M J 1973 *J. Phys. C: Solid State Phys.* **6** 1325
Catlow C R A, Norgett M J and Ross T A 1977 *J. Phys. C: Solid State Phys.* **10** 1627
Chadwick A V 1983 *Solid State Ion.* **8** 209
Corish J, Catlow C R A, Jacobs P W M and Ong S H 1982 *Phys. Rev.* B **25** 6425
Derrington C E, Lindner A and O'Keeffe M 1975 *J. Solid State Chem.* **15** 171
Dickens M H, Hayes W and Hutchings M T 1976 *J. Physique Coll.* **12** C7 353
Dixon M and Gillan M J 1980a *J. Phys. C: Solid State Phys.* **13** 1919
—— 1980b *J. Physique Coll.* **41** C6 24
Einstein A 1905 *Ann. Phys., Lpz.* **17** 549
Gillan M J and Dixon M 1980 *J. Phys. C: Solid State Phys.* **13** 1901
Matthews G E and Crawford J H 1977 *Phys. Rev.* B **15** 55
Rao K V and Smakula A 1966 *J. Appl. Phys.* **37** 319
Sangster M J L and Dixon M 1976 *Adv. Phys.* **25** 247
Sirdeshmukh D B and Deshpande V T 1964 *Indian J. Pure Appl. Phys.* **2** 405
Walker J 1982 *Springer Lecture Notes in Physics* vol 166, ed. C R A Catlow and W C Macrodt (Berlin: Springer)